Journal of Alloys and Compounds 643 (2015) S39–S45

Contents lists available at ScienceDirect

Journal of Alloys and Compounds

journal homepage: www.elsevier.com/locate/jalcom

Microstructure and texture characteristics of the metastable Fe–21Mn–3Si–3Al alloy after cold deformation

Joanna Kowalska [a,*], Wiktoria Ratuszek [a], Małgorzata Witkowska [a], Anna Zielińska-Lipiec [a], Tomasz Tokarski [b]

[a] AGH University of Science and Technology, Faculty of Metals Engineering and Industrial Computer Science, Av. Mickiewicza 30, 30-059 Cracow, Poland
[b] AGH University of Science and Technology, Faculty of Non-Ferrous Metals, Av. Mickiewicza 30, 30-059 Cracow, Poland

ARTICLE INFO

Article history:
Available online 20 April 2015

Keywords:
High manganese alloy
Deformation
Martensitic transformation
Microstructure
Texture

ABSTRACT

Cast Fe-21.2 Mn-2.99 Si-2.73 Al-0.02 wt.% C alloy ingot was homogenized at 1150 °C, hot-rolled at starting temperature 1000 °C, solution treated at 1150 °C for 1 h and cold-rolled to 56% thickness reduction. Metallographic and X-ray diffraction studies revealed that, for small degrees of deformation, ε martensite had nucleated within numerous stacking faults. EBSD analysis showed that α' martensite also formed within the ε plates. Plastic deformation occurred by mechanical twinning and martensitic transformations, both $\gamma \rightarrow \varepsilon$ and $\gamma \rightarrow \varepsilon \rightarrow \alpha'$ (TWIP and TRIP effect), with the Burgers (Shoji–Nishiyama) $\{0\,0\,0\,1\}\varepsilon||\{1\,1\,1\}\gamma$, $\langle 1\,1\,2\,0\rangle\,\varepsilon\,||\,\langle 1\,1\,0\rangle\,\gamma$ and Kurdjumov–Sachs $\{1\,1\,1\}\gamma||\{1\,1\,0\}\alpha$, $\langle 1\,1\,0\rangle\,\gamma||\langle 1\,1\,1\rangle\,\alpha$ relations between the austenite (γ), and martensite (ε and α').

1. Introduction

Construction materials have to possess, first and foremost, a good combination of strength and plasticity. In recent years, research into addition to steels of manganese, which is regarded as a very attractive alloying element, has been increasing [1–8], in particular, for the automotive industry. For the new generation of high-manganese steels, with Al and Si additions, it is possible to obtain reduction in mass, which, indirectly, causes a decrease in the emission of harmful gases into the atmosphere [1,9,10]. Fe–Mn–Si–Al alloys are used for car parts, which are intended to improve the safety of passengers in case of a collision, due to their good energy absorption capability [7,9]. Various deformation mechanisms may act, depending on stacking fault energy, SFE, namely: mechanical twinning (TWIP-effect), deformation-induced phase transformation (TRIP-effect); alternatively, shear bands (SBIP-effect) may be formed [1–4,11]. The value of SFE is influenced principally by chemical composition and temperature.

The metastable austenite γ (in alloys having a low SFE below 15 mJ/m^2) may form partly hexagonal ε martensite, or regular α' martensite, which significantly increases strengthening [1–4]. Thermodynamically stable austenite, the SFE of which amounts to between 20 and 30 mJ/m^2, in the course of plastic deformation may undergo mechanical twinning, which increases the strength and plastic properties of such alloys [5].

In general, manganese in high-manganese steels amounts to between 15 and 30 wt.% [5]. The addition of Al and Si to Fe–Mn alloys exerts an influence upon SFE, and, ipso facto, upon the phase stability of austenite and mechanical properties such as work hardening caused by phase transformation and deformation twinning [6,7]. The addition of Si decreases SFE and favours martensitic transformation, both in the course of cooling, and of deformation. Quite the opposite, Al causes an increase in SFE and strongly suppresses the martensitic transformation [1]. Carbon is an austenite stabilizer, and, in this group of steels does not exceed 0.6 wt.% [2]. The influence exerted by carbon in high-manganese steels upon martensitic transformation induced by cooling and deformation were broadly analysed in the papers of Seol and collaborators [8].

High-manganese steels are characterized by the TRIP effect when the manganese content is lower than 15 wt.%, whereas the TWIP effect dominates when the manganese content is greater than 25%. If manganese content is between 15 and 25 wt.%, then both mechanisms, TRIP and TWIP, occur simultaneously [6]. In the course of plastic deformation, metastable austenite may undergo transformation directly into α' martensite ($\gamma \rightarrow \alpha'$), or, undergo such a transformation through the intermediary phase of ε martensite, and, subsequently, into α' martensite: $\gamma \rightarrow \varepsilon \rightarrow \alpha'$ [12,13].

* Corresponding author. Tel.: +48 (12)617 30 28; fax: +48 (12)617 31 90.
E-mail address: joannak@agh.edu.pl (J. Kowalska).

http://dx.doi.org/10.1016/j.jallcom.2015.04.086
0925-8388/

The majority of studies of high-manganese alloys concerns TWIP, especially mechanical properties, whereas less attention has been paid to alloys in which both TRIP and TWIP effects can occur, and to the crystallographic texture forming in the course of deformation. It is indispensable to be acquainted with textures found in these materials, and with the influence exerted by them upon the processes of the formation of microstructure [4]. This, in particular the shape of grains and anisotropy, result in differences in properties. Anisotropy is of a significant importance in a number of technological processes, including plastic processing.

As a consequence of deformation, significant changes to the crystallographic orientation of the material take place. Cold plastic deformation occurs by slip and twinning, and in austenitic steels the phase transformation: $\gamma \rightarrow \varepsilon \rightarrow \alpha'$ may also occur. The formed texture is dependent, first and foremost, upon the chemical composition, the crystal structure, the initial orientation, the grain size and the parameters of plastic deformation [14,15]. There exists a close correlation between the factors determining the formation and development of the texture of deformation and stacking fault energy (SFE). In a high-manganese steel, if the stacking fault energy is small, the phase transformation ($\gamma \rightarrow \varepsilon \rightarrow \alpha'$) occurs during deformation. Crystallographic correlations between austenite and the products of the transformation (ε, α') constitute a significant aspect. The first relationship between austenite (γ) and martensite (α') was presented by Young in 1926, on the basis of X-ray analysis of meteorites. His crystallographic relationship is identical to a slightly later one, which is currently commonly referred to as the Kurdjumov–Sachs relationship (K–S) [16].

In a phase transformation, a single initial orientation, depending upon the symmetry and orientation of the parent crystal, has a certain number of final orientations, referred to as crystallographic variants. From the purely crystallographic point of view, all possible variants are equally likely to occur. Nevertheless, in practice, depending on a number of metallurgical and crystallographic parameters, a significant difference in the likelihood of the variants is observed. Not all theoretically possible orientations are observed in experiments. Very frequently, only certain orientations occur in the newly-formed phase resulting from the transformation. This phenomenon is referred to as crystallographic variant selection [17,18]. Different criteria of selection of particular variants, for example as being the consequence of: orientations, the actively-functioning slip systems, dislocation reactions, the shape and size of the grains of the parent phase, and the values of internal stresses have been taken under consideration [17,18].

Taking into account the fact that a phase transformation occurs in accordance with a determined variant, it is possible to predict the final texture of a material, if the initial texture is known. Whether a phase transformation occurs with the selection of a determined variant, or without variant selection (namely, with all variants equally likely), the transformed texture is, respectively, strong or broad.

In the course of the phase transformation of austenite into martensite, from the single grain of the parent phase, a different number of the crystals of martensite, having different crystallographic orientations, may be formed. Martensite orientations are related to the orientations of the parent grains of austenite by precisely-determined crystallographic relationships. Those relationships may be expressed either by stating precisely the determined axis and angles of rotation, or by means of mutually-corresponding planes and directions in the parent and product phases.

In this paper the principal objective of the research was to conduct a detailed analysis of microstructure and determine the crystallographic correlations between austenite (γ) and martensite (ε, α').

2. Material and methods

Fe-21.2 wt.% Mn, 2.99 wt.% Si, 2.73 wt.% Al and 0.02 wt.% C alloy was melted in a 100 kg VSG-100 PVA TePla AG vacuum induction furnace. The ingot was homogenized at 1150 °C for 4 h to reduce the segregation of the alloying elements, then hot-rolled with the starting temperature of 1000 °C from a plate of 60 mm thickness to 6 mm. Next the material was heated to 1150 °C, kept at this temperature for 1 h and water quenched. Then the plate thickness was reduced to 56% by rolling on a laboratory rolling mill at room temperature. The rolling direction was the same as that in hot-rolling.

Samples for X-ray diffraction were prepared by grinding to 4000 grit, subsequently mechanically-polished using 3, 1 and 0,5 μm diamond suspensions and finally electrolytically polished to remove the deformation layer. Central layers of samples were examined on a Bruker D8 Advance and a Siemens D500 diffractometers using $Co_{K\alpha}$ radiation ($_{k\alpha}$ = 0.179 nm) and $Cu_{K\alpha}$ radiation ($_{k\alpha}$ = 0.154 nm) for the measurement of texture and phase analysis, respectively. For austenite (γ), the incomplete pole figures of four planes were recorded ($\{111\}\gamma$, $\{200\}\gamma$, $\{220\}\gamma$, $\{311\}\gamma$), and so were five plane for ε martensite ($(10\bar{1}0)\varepsilon$, $(0002)\varepsilon$, $(10\bar{1}1)\varepsilon$, $(10\bar{1}2)\varepsilon$, $(11\bar{2}0)\varepsilon$), and three planes for α' martensite ($\{110\}\alpha'$, $\{200\}\alpha'$, $\{211\}\alpha'$). On the basis of the experimental pole figures, the calculated pole figures and fibres orientation for austenite $\alpha_{FCC} = \langle 110\rangle||ND$, $\tau_{FCC} = \langle 110\rangle||TD$, $\eta_{FCC} = \langle 001\rangle||RD$ and $\beta_{FCC} = \{110\}\langle 112\rangle$ through $\{123\}\langle 634\rangle$ to $\{112\}\langle 111\}$ were determined.

TEM and SEM samples were cut from a longitudinal section of the cold rolled sheet. Microstructural observations were conducted using a transmission electron microscope JEM 200XM and a Hitachi SU-70 field emission gun scanning electron microscope equipped with Thermo Scientific QUASOR EBSD system.

3. Results and discussion

Diffraction phase analysis of the initial state (0%) of Fe–21Mn–3Si–3Al alloy indicates that the structure of this alloy is composed of austenite (γ) with a small volume fraction of granular ferrite (δ), approximately 1.6% – the value determined by EBSD analysis. After cold rolling to 7% and 11% deformation, an increase in the peak intensity 200γ is observed (Fig. 1), which, subsequently, with an increase of deformation, undergoes weakening. In the case of larger deformations, X-rays diffraction patterns show diffraction lines, originating from ε martensite, which prove the occurrence of a martensitic transformation induced by deformation $\gamma \rightarrow \varepsilon$. After 18% deformation, the intensity of peaks originating from δ/α' (ferrite/martensite) $110\delta/\alpha'$, $200\delta/\alpha'$ and $211\delta/\alpha'$ rises as well. Weakening of the peaks originating from the ε phase, and an increase in the intensity of peaks originating from the δ/α' phase prove that the phase transformation induced by deformation occurs as follows: $\gamma \rightarrow \varepsilon \rightarrow \alpha'$ (Fig. 1). The qualitative phase analysis is made difficult because diffraction lines originating from the γ, δ/α' and ε phases, for certain angular ranges of 2θ, are located on one another (Fig. 1).

It has been previously shown [2–4,6–8,13] that the phase transformation occurs in the course of deformation. Depending upon the chemical composition, martensite with a hexagonal structure (ε) was formed [3], and was subsequently transformed into regular structure martensite (α').

Grässel et al. [2] and Frommeyer et al. [7] investigated manganese steels deformed at various temperatures. In deformed Fe-15Mn-3Si-3Al, the phase transformation $\gamma \rightarrow \varepsilon \rightarrow \alpha'$ occurred in the temperature range 80–150 °C [7]. In Fe–20Mn–3Si–3Al, deformed in the temperature range 50–200 °C, austenite became metastable, and a phase transformation took place. As a result of formation of martensite α', an increase in elongation and tensile strength occurred. The elongation increased with a decrease in temperature, related to the amount of the formed martensite. The volume fraction of martensite ε increased from 5% to 50% deformation, and subsequently, with deformation increase, it remained stable, and afterwards fell. The volume fraction of martensite α' increased throughout the entire range of deformations [2].

The analysis of texture was performed on the basis of calculated pole figures and orientation fibres (Figs. 2–4). These pole figures:

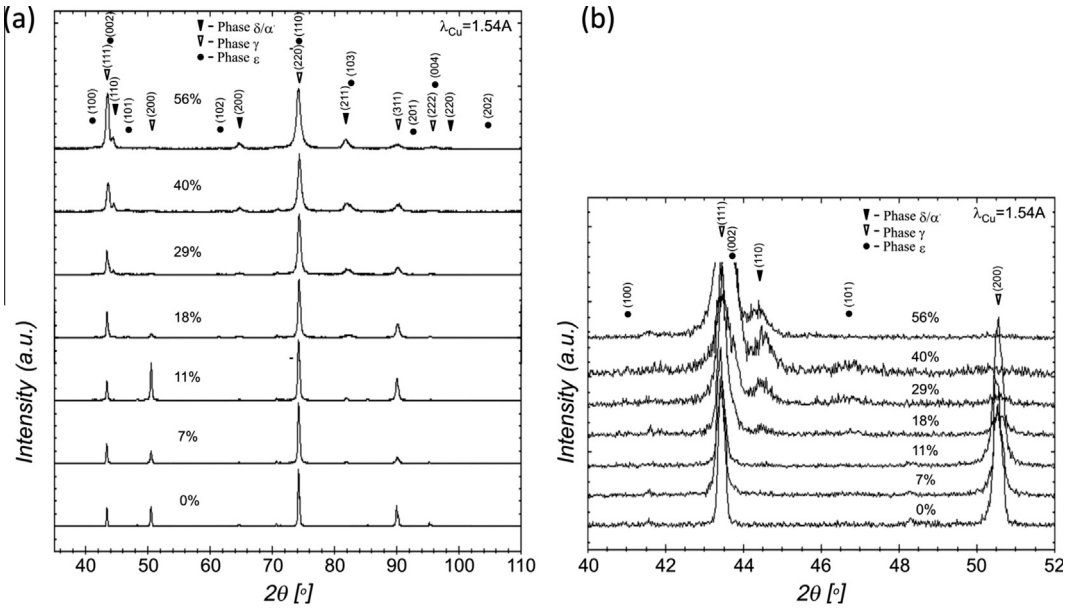

Fig. 1. X-ray diffractions patterns of the Fe–21Mn–3Si–3Al alloy in the initial state (0%) and after cold-rolling to reductions 7–56% (a), the expanded plot the (1 1 1) and (2 0 0) for austenite and the (0 0 2) and (1 0 1) for martensite ε peaks (b).

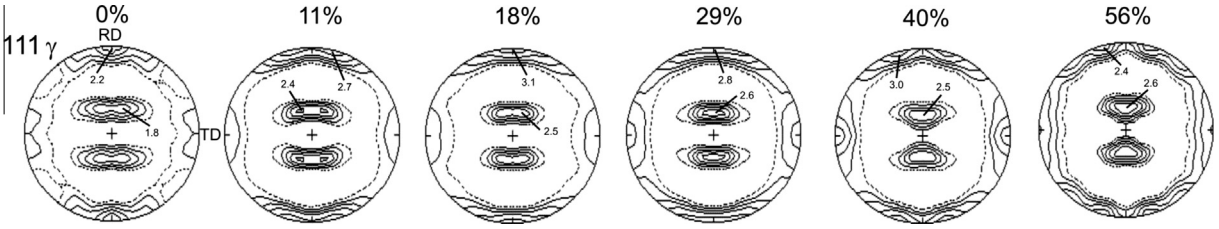

Fig. 2. Calculated pole figure 111 for austenite (γ) in the initial state (0%) and after cold-rolling to reductions 11–56%.

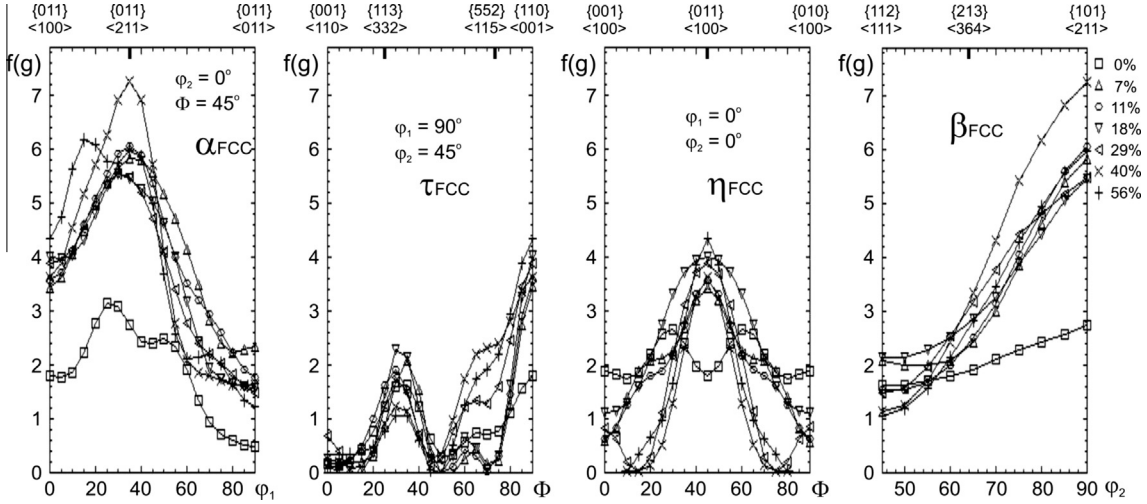

Fig. 3. Values of the orientation distribution functions $f(g)$ for austenite along the fibres $\alpha_{FCC} = \langle 1\,1\,0\rangle||ND$, $\tau_{FCC} = \langle 1\,1\,0\rangle||TD$, $\eta_{FCC} = \langle 0\,0\,1\rangle||RD$ and $\beta_{FCC} = \{1\,1\,0\}\langle 1\,1\,2\rangle$ through $\{1\,2\,3\}\langle 6\,3\,4\rangle$ to $\{1\,1\,2\}\langle 1\,1\,1\rangle$.

111γ for austenite, 002ε for ε martensite and $110\delta/\alpha'$ (ferrite/martensite) were chosen.

Austenite in its initial state (0%) was characterized by a comparatively weak texture. In its texture, the weakly limited α_{FCC} fibre, with the maximum matching the orientation $\{1\,1\,0\}\langle 1\,1\,3\rangle$ of the orientation of distribution function $f(g) = 3.1$, was made visible. Orientations such as the alloy type $\{1\,1\,0\}\langle 1\,1\,2\rangle$, $\{3\,5\,8\}\langle 1\,1\,1\rangle$ and a weak component of the Cu $\{1\,1\,2\}\langle 1\,1\,1\rangle$ (Figs. 2 and 3) type were observed. As deformation increased to 40%, increase in the component intensities of texture in the α_{FCC} fibre was observed. The maximum value $f(g)$ for deformations in the range 7–40% matches the orientation:

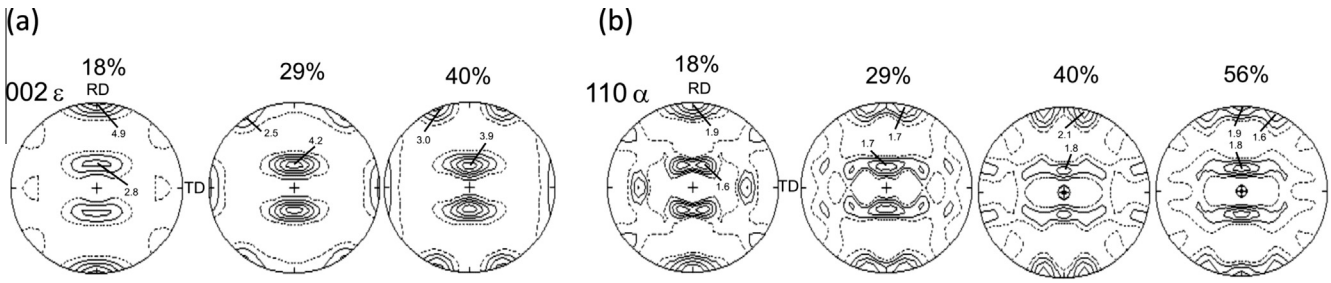

Fig. 4. Calculated pole figure 002 for martensite ε after cold-rolling 18–40% (a) and 110 for martensite α' after cold-rolling 18–56% (b).

$\{110\}\langle 112\rangle$. After 29%, the component of the texture $\{112\}\langle 111\rangle$ (Fig. 3) disappeared, and after 56%, movement of the maximum $f(g)$ in the α_{FCC} fibre to the orientation of $\{110\}\langle 115\rangle$ was observed (Fig. 3). For the entire range of the deformations, austenite had a partly fibrous texture (Figs. 2 and 3).

Fig. 4a shows the calculated pole figures 002 for ε martensite for deformations of 18, 29 and 40%. After 18% deformation, the texture of ε martensite was comparatively strong, with the maximum located in RD and matching the plane $(10\bar{1}0)$. On the pole figure 002ε, there is a strong component $(10\bar{1}3)$ at the distance of 32° from ND. After 29% deformation, the maximum moved from RD in the direction of ND to the orientation $(10\bar{1}4)$ at the distance of 26° from ND. Orientations, the maximum intensity of which is in RD, have disappeared. As the degree of deformation increases, the weakening of the main components of the texture of ε martensite is observed. The texture is of a similar character in the entire range of deformations (Fig. 4a).

Fig. 4b shows the measurements of texture for α' martensite. For the small degrees of deformation (7% and 11%), it proved impossible to measure texture due to the insignificant volume fraction of this phase. Clear diffraction lines only appear after deformation by 18%. The texture of α' martensite in the entire range is comparatively weak, and has a partly fibrous character.

Lü et al. [3] researched the development of texture in a cold-rolled high-manganese steel. Similarly, at the initial stage of deformation they observed in austenite an increase in the component intensity of the texture of the S $\{112\}\langle 634\rangle$ and Cu $\{112\}\langle 111\rangle$ types, and afterwards, with an increase in the deformation, a decrease in the intensity of these components. The transformation of the texture of the Cu type into the texture of the brass $\{110\}\langle 112\rangle$ type was recorded also by others [3,13,19,20]. The development of the brass component is the consequence of a non-homogeneous deformation promoted by the formation of deformation twins. The components of the Cu and S types are orientations favouring the formation of martensite ε in the plane of rolling. For that very reason, weakening, or even disappearance, of those components occurs with an increasing deformation. The presence (of the second phase) of martensite above a certain critical value exerts a significant influence upon the development of texture of steel [20].

Figs. 5 and 6 show microstructures obtained with the use of EBSD. These observations showed that, soon after 11% deformation, transformation of austenite into ε martensite ($\gamma \rightarrow \varepsilon$) occurs. In austenite grains laths of ε martensite with small precipitates of phase having a body-centred cubic structure (bcc) were observed. This indicates that the transformation of ε martensite into α' martensite has occurred during the deformation. In the structure before the deformation, a large bcc precipitate, the initial ferrite (δ), was observed (Fig. 5). Analysing the pole figures of the planes $\{111\}\gamma$ and $\{001\}\varepsilon$, it is possible to ascertain the crystallographic correlations between the phases γ and ε, which were for the first time reported by Burgers $\{0002\}\varepsilon||\{111\}\gamma$ [21]. At present this correlation is termed the Shoji–Nishiyama relation (S–N): $(111)\gamma||(0001)\varepsilon$ and $[1\bar{1}0]\gamma||[11\bar{2}0]\varepsilon$ [22]. The relation between certain orientations of austenite (γ) and martensite (α') is described by the Kurdjumov–Sachs relationship (K–S): $\{111\}\gamma||\{101\}\alpha'$ and $\langle 101\rangle\ \gamma||\langle 111\rangle\ \alpha'$ (which was marked with a circle in Fig. 5e–g). It is possible to notice that not all the variants were implemented, and that the transformation is by a variant selection.

After 29% deformation, in the EBSD map of the alloy austenite and α' martensite were identified (Fig. 6). The structure has a banded character. The occurrence of the Kurdjumov–Sachs relationship between the γ and α' phases was determined (Fig. 6d and e).

Similar crystallographic correlations between austenite (γ) and martensite (ε, α') have been reported [3,4,6,8,13,21,22]. In Ref. [3] transformation occurring by means of $\gamma \rightarrow \varepsilon$ is reported and the variant selection was of a selective character. Martensite ε behaved as the hard phase. Lui et al. [4] investigated the transformation: $\gamma \rightarrow \varepsilon \rightarrow \alpha'$ occurring in the course of cooling and deformation. In the case of a thermally-induced martensitic transformation, a variant selection did not occur, the consequence of which was a refinement of the structure. In the case of a deformation-induced transformation, a variant selection occurred, which exerted a small influence upon grain refinement. It was observed [4] that the grains which had undergone the martensitic transformation had orientations situated close to the $\langle 100\rangle\ \gamma$ orientation in a basic triangle. For the majority of changes in which a transformation did not occur, orientations were observed in which the axis of compression was close to $\langle 110\rangle$. In turn, Seol et al. [8], reported, for high-manganese steel samples after tensile testing, the occurrence of the following crystallographic correlations between the phases: γ, ε α' $(111)\gamma||(0001)\varepsilon||(110)\alpha'$ and $\langle 1\bar{1}0\rangle\ \gamma||\langle 11\bar{2}0\rangle\varepsilon||\langle 1\bar{1}1\rangle\ \alpha'$ or $\langle 11\bar{2}\rangle\gamma||\langle 1100\rangle\ \varepsilon||\langle 110\rangle\ \alpha'$, which corresponded with the relationships: Shoji–Nishiyama (S–N), Kurdjumov–Sachs (K–S) or Nishiyama–Wassermann (N–W).

TEM microstructures confirm X-ray phase analyses, and also EBSD data. In the deformed material, numerous stacking faults are observed, and they occur individually (Fig. 7a and b), or are aggregated, making bands (bundles) and leading to formation of the ε phase. An increase in deformation causes a change in this mechanism. Austenite is dominated by deformation twins (Fig. 8a). ε martensite plates are observed after 29% deformation (Fig. 8b). Increasing the deformation to 56% causes an increase in the quantity of α' martensite (Fig. 9) and the ε phase is not observed.

It was previously shown that in austenite, with a significant tendency to form stacking faults, ε phase is formed as the consequence of the transformation [3,4,6,8,21,22]. The nucleation of martensite ε by means of stacking faults and partial dislocations a $\langle 112\rangle/6$ and the direct overlaying of stacking faults were observed [6]. The transformation: $\gamma \rightarrow \varepsilon$ frequently precedes the

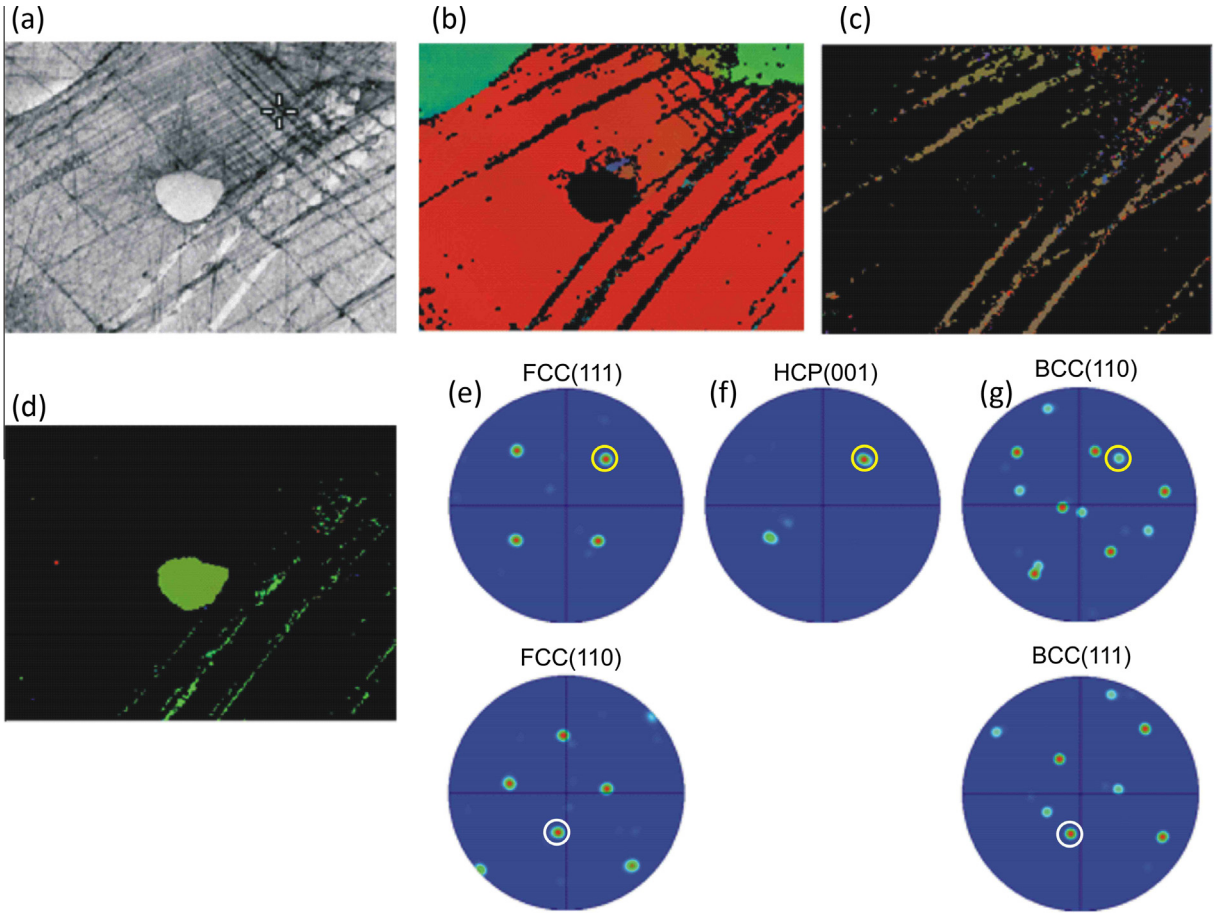

Fig. 5. EBSD phase maps for Fe–21Mn–3Si–3Al alloy after 11% cold-rolling (a) pattern quality, (b) austenite (γ-FCC), (c) martensite (ε-HCP), (d) ferrite/martensite (δ/α'-BCC), (e) pole figures of γ phase, (f) pole figure of ε phase, (g) pole figures of δ/α' phase.

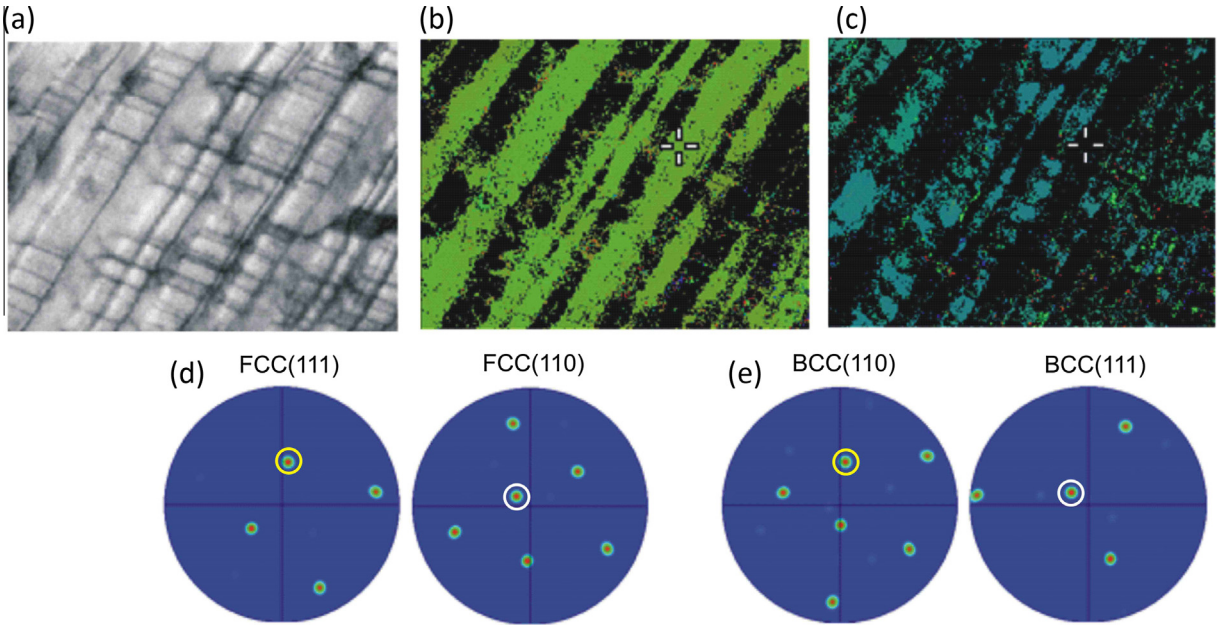

Fig. 6. EBSD phase maps for Fe–21Mn–3Si–3Al alloy after 29% cold-rolling (a) pattern quality, (b) austenite (γ-FCC), (c) ferrite/martensite (δ/α'-BCC), (e) pole figures of γ phase, (e) pole figures of α' phase.

transformation: $\varepsilon \rightarrow \alpha'$. Phase ε is, therefore, an intermediary state in the transformation of austenite into martensite α' [21]. Phase ε increases at the initial stage of deformation [6,21], and it subsequently undergoes a transformation into martensite α'. This

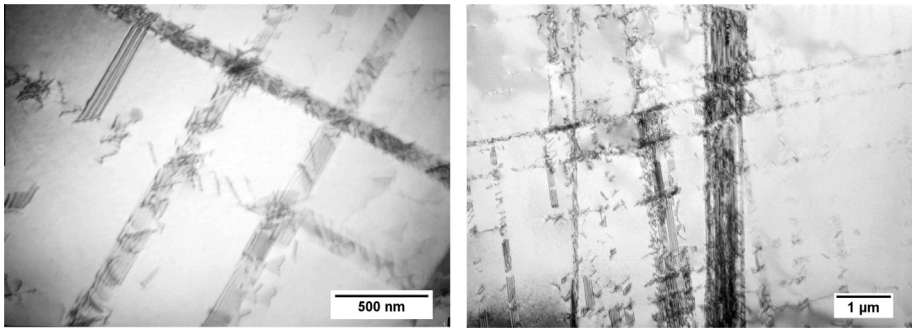

Fig. 7. TEM micrographs of Fe–21Mn–3Si–3Al alloy after 11% cold-rolling.

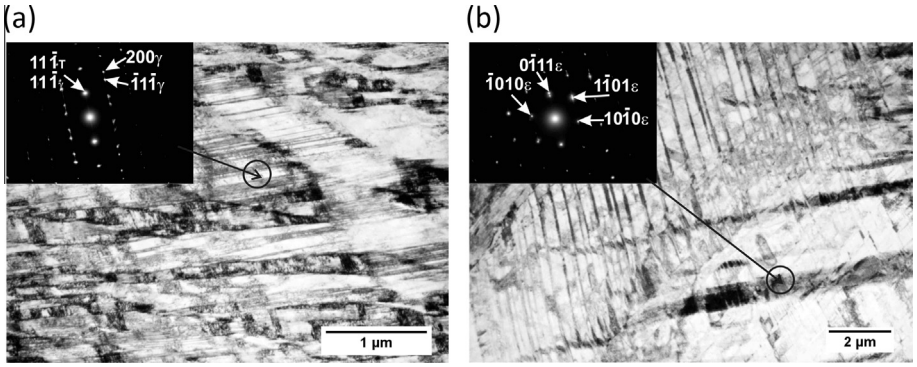

Fig. 8. TEM micrographs of Fe–21Mn–3Si–3Al alloy after 29% cold-rolling and SADPs taken from areas indicated by a circle (a) BF – diffraction pattern $[011]\gamma$, (b) BF – diffraction pattern $[1\bar{2}1\bar{3}]\varepsilon$.

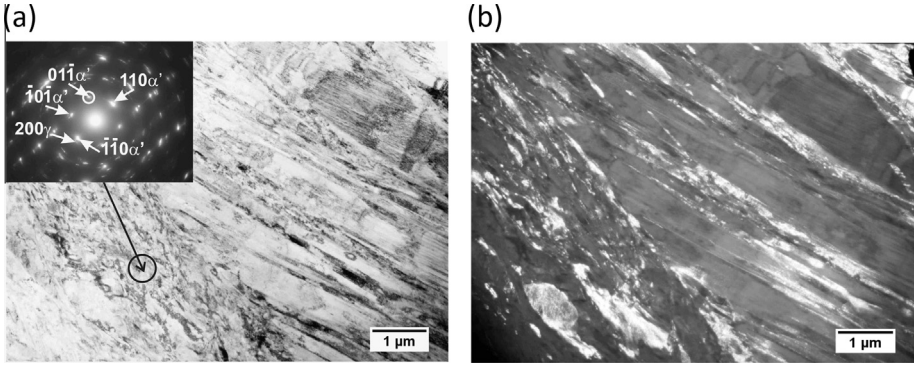

Fig. 9. TEM micrographs of Fe–21Mn–3Si–3Al alloy after 56% cold-rolling and SADPs taken from areas indicated by a circle (a) BF, (b) DF with $(01\bar{1})\alpha'$, diffraction pattern $[11\bar{1}]\alpha'$.

explains the lack of phase ε after 56% deformation, now reported. For the formation of martensite α' in the course of a deformation, it is indispensable for the two plates of phase ε or for a plate with a twin boundary [4,6,13,21] to form a cross-cut.

4. Summary

Upon the basis of X-ray diffraction, transmission electron microscopy (TEM) and electron backscattered diffraction (EBSD) experimental data on a cold-rolled high-manganese steel, the following conclusions have been reached:

1. In the course of deformation of Fe–21Mn–3Si–3Al steel, a number of mechanisms operate, namely deformation of the initial phase (austenite), the formation, and also the deformation, of new phases (martensite ε and α'), both by slip and twinning.
2. The texture of austenite in the initial state is weak and during deformation develops in the direction of a texture typical for alloys having a low stacking fault energy, i.e. $\{110\}\langle 112\rangle$ alloy type.
3. Diffraction analyses and scanning electron microscopy showed these crystallographic relationships between the phases austenite (γ) and martensite (ε and α'): $(111)\gamma||(0001)\varepsilon||(110)\alpha'$ and $\langle 101\rangle\ \gamma||\langle 11\bar{2}0\rangle\ \varepsilon||\langle 111\rangle\ \alpha'$.

Acknowledgments

This work was sponsored by the Polish National Science Centre under Contract no 2011/01/D/ST8/03905.

Appreciation is also expressed to Prof. A.S. Wronski (University of Bradford, UK), who edited the text.

References

[1] B.X. Huang, X.D. Wang, Y.H. Rong, L. Wang, L. Jin, Mechanical behavior and martensitic transformation of an Fe-Mn-Si-Al-Nb alloy, Mater. Sci. Eng., A 438–440 (2006) 306–311.

[2] O. Grässel, L. Krüger, G. Frommeyer, L.W. Meyer, High strength Fe-Mn-(Al, Si) TRIP/TWIP steels development-properties-application, Int. J. Plast 16 (2000) 1391–1409.

[3] Y. Lü, B. Hutchinson, D.A. Molodov, G. Gottstein, Effect of deformation and annealing on the formation of ε-martensite in an Fe-Mn-C alloy, Acta Mater. 58 (2010) 3079–3090.

[4] T.-Y. Lui, P. Yang, L. Meng, F.-Y. Lu, Influence of austenitic orientation on martensitic transformations in a compressed high manganese steel, J. Alloy. Compd. 509 (2011) 8337–8344.

[5] L. Chen, S.-J. Lee, B.C. de Cooman, Mechanical properties of H-charged Fe-18Mn-1.5Al-0.6C TWIP steel, ISIJ Int. 52 (9) (2012) 1670–1677.

[6] H. Ding, H. Ding, D. Song, Z. Tang, P. Yang, Strain hardening behavior of TRIP/TWIP steel with 18.8% Mn, Mater. Sci. Eng. A 528 (2011) 868–873.

[7] G. Frommeyer, U. Brüx, P. Neumann, Supra-ductile and high-strength manganese-TRIP/TWIP steels for high energy absorption purposes, ISIJ Int. 43 (3) (2003) 438–446.

[8] J.-B. Seol, J.E. Jung, Y.W. Jang, C.G. Park, Influence of carbon content on the microstructure, martensitic transformation and mechanical properties in austenite/ε-martensite dual-phase Fe-Mn-C steels, Acta Mater. 61 (2013) 558–578.

[9] G. Frommeyer, U. Brüx, Microstructure and mechanical properties oh high-strength Fe-Mn-Al-C ligh-weight TRIPLEX steels, Steel Res. Int. 9–10 (2006) 627–633.

[10] L. Samek, D. Krizan D, Steel-Material of Choice for Automotive Lightweight Applications, Metal 2012, Czech Republic.

[11] S. Alain, J.-P. Chateau, O. Bouaziz, S. Migot, N. Guelton, Correlations between the calculated stacking fault energy and the plasticity mechanisms in Fe-Mn-C alloys, Mater. Sci. Eng., A 387–389 (2004) 158–162.

[12] A. Sato, K. Soma, T. Mori, Hardening due to pre-existing ϵ-Martensite in an Fe-30Mn-1Si alloy single crystal, Acta Metall. 30 (10) (1982) 1901–1907.

[13] J. Kowalska, W. Ratuszek, M. Witkowaska, A. Zielińska-Lipiec, Influence of cold plastic deformation on the development of the texture of high-manganese austenitic steel, Solid State Phenom. 203–204 (2013) 115–120.

[14] C. Donadille, R. Valle, P. Dervin, R. Penelle, Development of texture and microstructure during cold-rolling and annealing of fcc alloys: example of austenitic stainless steel, Acta Metall. 37 (6) (1989) 1547–1571.

[15] K. Lücke, O. Engler, Effect of particles on development of microstructure and texture during rolling and recrystallization in fcc alloys, Mater. Sci. Technol. 6 (1990) 1113–1130.

[16] Y. He, S. Godet, P.J. Jacques, J.J. Jonas, Crystallographic relationship between fcc and bcc crystals: a study using EBSD techniques, Solid State Phenom. 105 (2005) 121–126.

[17] M.P. Butrón-Guillén, C.S. Da Costa Viana, J.J. Jonas, A variant selection model for predicting the transformation texture of deformed austenite, Metallurg. Mater. Trans. A 28A (1997) 1755–1768.

[18] M. Sum, J.J. Jonas, A dislocation reaction model for variant selection during the austenite-to-martensite transformation, Text. Microstruct. 31 (1999) 187–215.

[19] S. Vercammen, B. Blanpain, B.C. De Cooman, P. Wollants, Cold rolling behaviour of an austenitic Fe–30Mn–3Al–3Si TWIP-steel: the importance of deformation twinning, Acta Mater. 52 (2004) 2005–2012.

[20] B. Ravi, B. Kumar, N.R. Mahato, D.K. Bandyopadhyay, Bhattacharya, comparison of rolling texture in low and medium stacking fault energy austenitic stainless steels, Mater. Sci. Eng., A 394 (2005) 296–301.

[21] S. Gorczyca, Phase transformation ε-γ as a process previous to the recrystallization of cold worked chromium-manganese austenitic steel, Sci. Bull. Acad. Min. Metall. 187 (1967).

[22] W. Zhang, Z. Liu, Z. Zhang, G. Wang, The crystallographic mechanism for deformation induced martensitic transformation observed by high resolution transmission electron microscope, Mater. Lett. 91 (2013) 158–160.